ELSEVIER

Journal of Power Sources 56 (1995) 25–30

JOURNAL OF POWER SOURCES

Effects of lithium content on the electrochemical lithium intercalation reaction into $LiNiO_2$ and $LiCoO_2$ electrodes

Young-Min Choi [a], Su-Il Pyun [a], Joon-Sung Bae [a], Seong-In Moon [b]

[a] *Department of Materials Science and Engineering, Korea Advanced Institute of Science and Technology, 373-1 Kusung-Dong, Daejon 305-701, South Korea*

[b] *Division of Electrical Materials, Korea Electrotechnology Research Institute, 28-1 Sungju-Dong, Changwon 641-600, South Korea*

Received 7 January 1995; accepted 10 February 1995

Abstract

The electrochemical lithium intercalation reaction into $LiNiO_2$ and $LiCoO_2$ electrodes in 1 M $LiClO_4$–propylene carbonate solution is investigated as a function of lithium content in the oxide electrodes by using X-ray diffractometry (XRD), electrochemical impedance spectroscopy (EIS), and a galvanostatic intermittent titration technique (GITT). $Li_{1-\delta}NiO_2$ shows a greater loss in capacity during the first intermittent discharge, as well as a higher resistance for the electrochemical intercalation reaction, in comparison with $Li_{1-\delta}CoO_2$. This is attributed to a partial cation mixing in $Li_{1-\delta}NiO_2$ which is substantiated by XRD studies. The electrochemical impedance spectra of the $Li_{1-\delta}NiO_2$ electrode reveals that the magnitude of the intermediate frequency arc that is associated with the absorption reaction decreases with increasing lithium content, $(1-\delta)$, in the range from 0.5 to 0.7. By contrast, $Li_{1-\delta}CoO_2$ exhibits the reverse behaviour. The component diffusivities of lithium ions display a nearly constant value, in the order of 10^{-11} cm^2 s^{-1}, for both electrodes at room temperature, irrespective of the value of $(1-\delta)$ over the range 0.5–0.7. It is suggested that lithium-ion diffusion through both the layered oxides is affected by the number of empty sites within the lithium-ion layer, and not by the lattice parameter.

Keywords: Lithium intercalation; Layered oxide; Lattice constant; Electrochemical impedance; Lithium diffusion

1. Introduction

In both rechargeable lithium battery systems and electrochromic material systems, the respective discharge/charge and colouring/bleaching reactions involve the intercalation/de-intercalation of lithium ions into/from the corresponding cathode and electrochromic materials [1,2]. Layered transition metal chalcogenides and oxides, both with a layer of transition metal atom sandwiched between two layers of chalcogen or oxygen atoms, are very attractive cathode materials [3]. Because of their mixed electronic/ionic conductivity and weak interlayer force, lithium ions can intercalate reversibly between the layers of the both materials.

In order to tackle the problems associated with the safety and the dendritic growth of lithium metal anodes upon cycling, a more advanced approach is being pursued [4]. This employs strongly oxidizing compounds that are capable of reversibly intercalating lithium ions above 4 V_{Li/Li^+} as cathode materials. Layered transition metal oxides such as $LiNiO_2$ [5–7] and $LiCoO_2$ [8–10] are known to satisfy this requirement. $LiCoO_2$ has received more attention than $LiNiO_2$ because it is easier to prepare and provides a higher cell voltage. According to previous reports [6,7], even a small cation mixing in $LiNiO_2$ influences electrochemical properties of the electrode, such as the working voltage and the rechargeable capacity.

Over the past few decades, most studies of the intercalation/de-intercalation reaction of lithium ions into layered intercalation compounds have been devoted to the diffusion of lithium ions within the compounds and have assumed that the diffusion is the rate-controlling process [11,12]. If the cathode materials provide a high lithium-ion mobility, however, a process such as charge transfer or absorption at the electrolyte/electrode interface may be the rate-determining step. Moreover, it has been reported [8,9] that the interfacial processes at the layered oxide electrode become increasingly important as the lithium content increases. Therefore, kinetic studies at different lithium contents should give a better understanding of the electrochemical intercalation reaction into $LiNiO_2$ and $LiCoO_2$ and its practicality as an innovative rechargeable battery system.

The present work is concerned with the interfacial reaction and the transport of lithium through $Li_{1-\delta}NiO_2$ and $Li_{1-\delta}CoO_2$ electrodes in 1 M $LiClO_4$–propylene carbonate

SSDI 0378-7753(95)02206-V

(PC) solution with various lithium contents. Consideration is also given to the effect of cation mixing in $Li_{1-\delta}NiO_2$ on the electrochemical intercalation reaction of lithium into the electrode. For this purpose, both electrochemical impedance spectra (EIS) and X-ray diffraction (XRD) patterns are obtained for the $Li_{1-\delta}NiO_2$ and $Li_{1-\delta}CoO_2$ electrodes as a function of lithium content. The chemical and component diffusivities of lithium ions in the oxide electrodes are determined as a function of lithium content by using a galvanostatic intermittent titration technique (GITT).

2. Experimental

$LiNiO_2$ powder was prepared by calcinating a pressed mixture of $LiOH \cdot H_2O$ and $Ni(OH)_2$ at 600 °C for 6 h in air, followed by heating in air at 700 °C for 12 h. Similarly, a pressed mixture of Li_2CO_3 and Co was calcinated at 600 °C for 12 h in air, and then heated in air at 900 °C for 24 h, to prepare $LiCoO_2$ powder.

The resulting products were ground to below 200 mesh (<75 μm in particle size) by using an agate mortar and pestle. The crystal structures of $LiNiO_2$ and $LiCoO_2$ were characterized by XRD. The powder XRD patterns were recorded on an automated Rigaku diffractometer that used Cu Kα radiation.

Cathode specimens were prepared by mixing $LiMO_2$ (M ≡ Ni, Co) powder with 5 wt.% Vulcan XC-72 carbon black. This mixture was stirred in NMP (*n*-methylpyrrolidone) and a binder solution of PVDF (polyvinylidene fluoride) was added in order to give a syrupy viscosity. The amount of binder solution was adjusted to 2 wt.% PVDF in the final cathode specimen. The slurry was spread on 316 stainless-steel ex-met. Upon evaporation of the NMP, the cathode specimens were dried under vacuum for 24 h.

A three-electrode electrochemical cell was employed for both the galvanostatic intermittent charge/discharge experiments and the electrochemical impedance measurements. The reference and counter electrodes were constructed from lithium foil, and a 1 M $LiClO_4$–PC solution was used as the electrolyte. PC as a solvent was dried for at least 24 h with previously activated 5 A molecular sieves. The lithium perchlorate ($LiClO_4$) solute was dried under vacuum at 120 °C for 12 h.

Galvanostatic intermittent charge/discharge curves were obtained under constant-current conditions by using an EG&G Model 273 potentiostat/galvanostat. The charge and discharge currents were selected so that a change in lithium content of $\Delta\delta = 1$ for $Li_{1-\delta}MO_2$ would occur during 10 h.

Electrochemical impedance measurements were performed with a Solartron 1255 frequency response analyser combined with a Solartron 1286 electrochemical interface under remote control by IBM-compatible personal computer. After the electrode attained an equilibrium potential, the electrochemical impedance measurements were carried out galvanostatically over frequencies between 10^{-3} and 10^5 Hz. All the electrochemical experiments were conducted at room temperature in a glove box (VAC HE493) that was filled with purified argon gas.

3. Results and discussion

3.1. XRD characterization of $LiNiO_2$ and $LiCoO_2$

Fig. 1(a) and (b) shows the XRD patterns for $LiNiO_2$ and $LiCoO_2$ powder prepared from hydroxide and carbonate salts, respectively. All peaks can be indexed by a hexagonal unit cell with lattice constants $a = 2.886$ Å, $c = 14.214$ Å for $LiNiO_2$, and $a = 2.816$ Å, $c = 14.046$ Å for $LiCoO_2$.

The structure of $LiMO_2$ (M ≡ Ni, Co) is based on a close-packed network of oxygen anions with ordering of the Li^+ and M^{3+} ions on alternating (111) planes of a cubic rock-salt structure. The (111) ordering introduces a slight distortion of the lattice to hexagonal symmetry. Hence, $LiMO_2$ crystallizes in a layered rock-salt structure with space group $R\bar{3}m$ [13]. The lattice constants of $LiNiO_2$ ($R\bar{3}m$) with a layered structure are very close to those of $LiNiO_2$ ($Fm\bar{3}m$) with a cubic structure. The latter is inactive in non-aqueous lithium cells. Therefore, cation mixing of Li^+ and Ni^{3+} ions between octahedral 3(*a*) and 3(*b*) sites occurs readily without any dimensional mismatch, and even a small amount of cation mixing affects the electrochemical properties of the cathode specimen, such as the rechargeable capacity and the resistance for electrochemical intercalation reaction.

The cation mixing in $LiNiO_2$ ($R\bar{3}m$) with a layered structure weakens the intensity of the (003) peak, whereas it

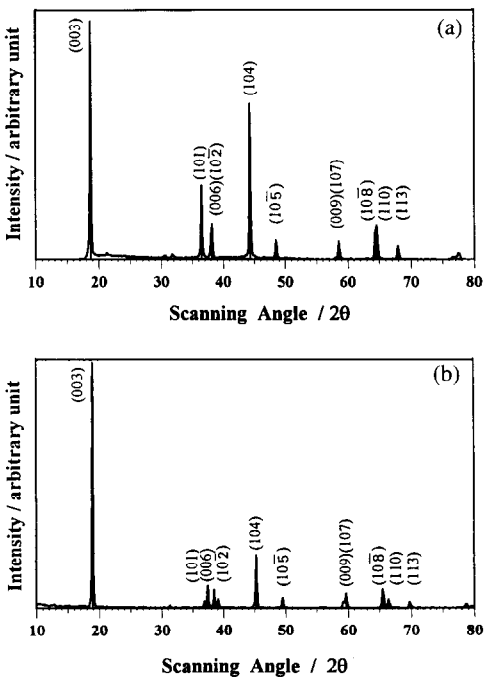

Fig. 1. X-ray diffraction patterns of (a) $LiNiO_2$ and (b) $LiCoO_2$. The Miller indices of the Bragg peaks are indicated over each peak.

scarcely influences the intensity of the (104) peak. Therefore, the X-ray intensity ratio, $I_{(003)}/I_{(104)}$, can be regarded as a simple criterion for estimating the degree of cation mixing $LiNiO_2$ ($R\bar{3}m$). It has been reported that $LiNiO_2$ is electrochemically inactive and that it is difficult to distinguish the ($10\bar{8}$) and (110) peaks from each other when the ratio is below 1.2 [6,7]. Given the value of I_{003}/I_{104} of that is 1.31 calculated from the XRD pattern (Fig. 1(a)) and the clear separation of the ($10\bar{8}$) and (110) peaks, the $LiNiO_2$ prepared in this work is expected to be electrochemically active. By contrast, the electrochemical reactivity of $LiNiO_2$ should be poor because of partial cation mixing.

3.2. Galvanostatic intermittent charge/discharge curves for $LiNiO_2$ and $LiCoO_2$

Fig. 2(a) and (b) presents the first galvanostatic intermittent charge and discharge curves of $Li_{1-\delta}MO_2$ (M ≡ Ni, Co) as a function of intercalated lithium content, $1-\delta$, in 1 M $LiClO_4$/PC solution. The deviation from the ideal stoichiometry of $LiMO_2$, δ, was calculated from the values of the mass of the oxide, and of the electrical charge that is transferred during the application of current pulses.

The charge/discharge curves display a wide potential plateau near 3.6 V_{Li/Li^+} for $Li_{1-\delta}NiO_2$ and 3.9 V_{Li/Li^+} for $Li_{1-\delta}CoO_2$. The occurrence of this plateau is due to the coexistence of two pseudo-phases, namely, a diluted phase and a concentrated phase. As lithium de-intercalates from $Li_{1-\delta}NiO_2$ or $Li_{1-\delta}CoO_2$, Ni^{3+} or Co^{3+} ions are oxidized to unstable Ni^{4+} or Co^{4+} ions around the potential plateau [10]. A high concentration of Ni^{4+} or Co^{4+} is most likely to reduce the cathode crystallinity and, hence, the reversibility of the cell. The occurrence of the broad XRD peaks for $Li_{1-\delta}NiO_2$ and $Li_{1-\delta}CoO_2$ at $1-\delta<0.4$ can also be explained by this effect.

As shown in Fig. 2, in comparison with $Li_{1-\delta}CoO_2$, $Li_{1-\delta}NiO_2$ suffers a greater loss in capacity during the first intermittent discharge, as well as a greater instantaneous *IR* drop due to the increased resistance for the electrochemical intercalation reaction. This is attributed to a partial cation mixing in $Li_{1-\delta}NiO_2$, as discussed above.

3.3. Variation of lattice constants with lithium content

Fig. 3(a) and (b) presents the lattice constants, *a* and *c*, of both $LiNiO_2$ and $LiCoO_2$ as a function of intercalated lithium content, $1-\delta$. The lattice constant *a* increases monotonously with lithium content for both $Li_{1-\delta}NiO_2$ and $Li_{1-\delta}CoO_2$. The value of *c* remains nearly constant for

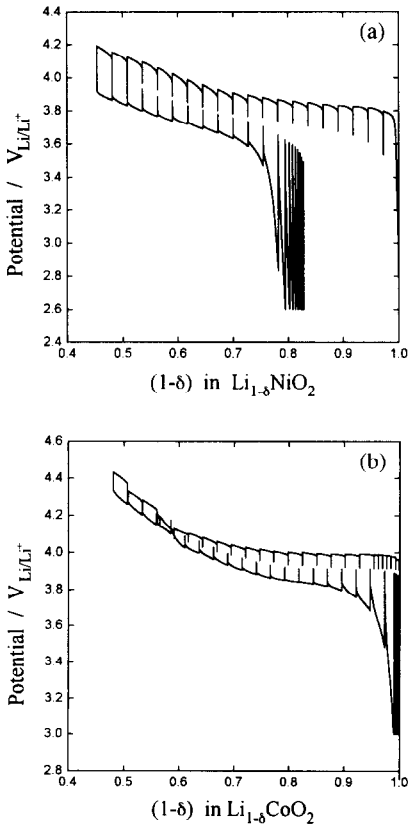

Fig. 2. First galvanostatic intermittent charge/discharge curves for Li/1 M $LiClO_4$–PC solution: (a) $Li_{1-\delta}NiO_2$, and (b) $Li_{1-\delta}CoO_2$ cell. Charge and discharge at the 10 h rate.

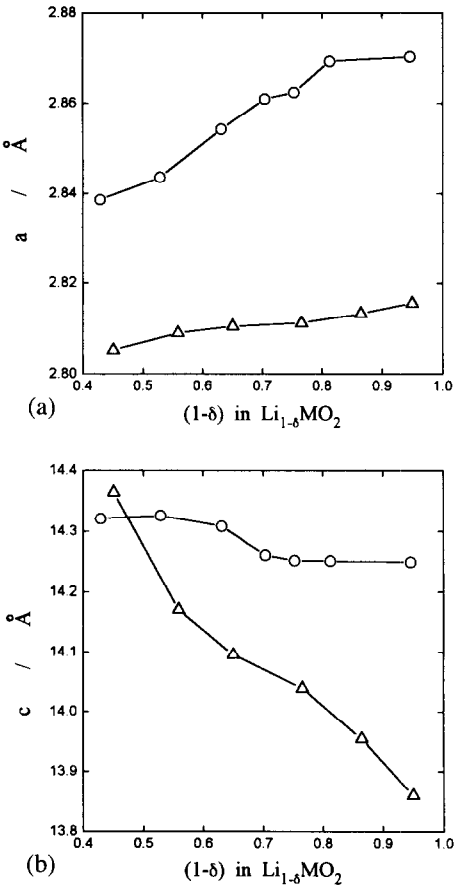

Fig. 3. Hexagonal lattice constants, *a* and *c*, of (○) $Li_{1-\delta}NiO_2$ and (△) $Li_{1-\delta}CoO_2$ as function of lithium content, $1-\delta$: (a) *a*-value, and (b) *c*-value.

$Li_{1-\delta}NiO_2$ irrespective of lithium content, but decreases monotonously for $Li_{1-\delta}CoO_2$.

In lithium intercalation compounds, the lattice constants can generally be influenced through elastic strain produced by intercalated lithium ions on the one hand, and coulombic attraction between lithium and oxygen ions on the other hand. For $Li_{1-\delta}CoO_2$ and $Li_{1-\delta}NiO_2$, the coulombic attraction energy effect is dominant over the elastic strain energy effect and this may account for the ionic bonding between the cobalt/nickel and the oxygen ions. The decrease in the lattice constant c of $Li_{1-\delta}CoO_2$ with increasing lithium is considerably more than that observed with $Li_{1-\delta}NiO_2$. This is due to the partial cation mixing in $Li_{1-\delta}NiO_2$, as mentioned above.

3.4. Electrochemical impedance spectroscopy

Figs. 4 and 5 present typical impedance spectra, in Nyquist presentation, for $Li_{1-\delta}NiO_2$ and $Li_{1-\delta}CoO_2$ electrodes, respectively, at various lithium contents in 1 M $LiClO_4$/PC solution. Below $1-\delta=0.8$, the impedance spectra of $Li_{1-\delta}NiO_2$ and $Li_{1-\delta}CoO_2$ electrodes consist of two separated arcs in the high and intermediate frequency range of 1 Hz to 100 kHz, and a line inclined at approximately 45° to the real axis in the low frequency range of 1 mHz to 1 Hz. The two arcs in the higher frequency range are due to reactions at the interface of the electrolyte/oxide electrode, while the inclined line in the lower frequency range is attributable

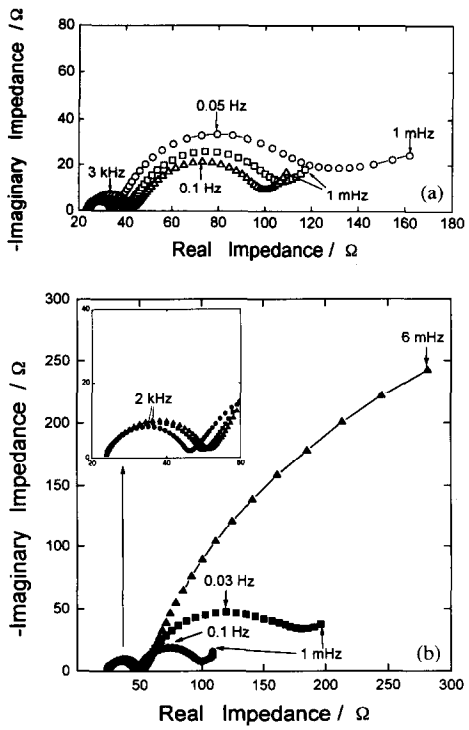

Fig. 4. Nyquist plots for $Li_{1-\delta}NiO_2$ electrode in 1 M $LiClO_4$–PC solution as function of lithium content, $1-\delta$: (a) (○) 0.5; (□) 0.6, and (△) 0.65; (b) (●) 0.7; (■) 0.8, and (▲) 0.85. Apparent exposed area of electrode = 2 cm^2.

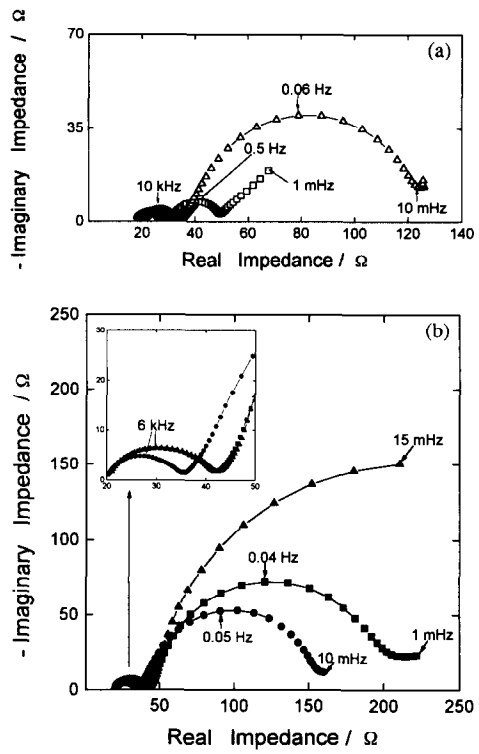

Fig. 5. Nyquist plots obtained from $Li_{1-\delta}CoO_2$ electrode in 1 M $LiClO_4$–PC solution as function of lithium content, $1-\delta$: (a) (○) 0.5; (□) 0.6, and (△) 0.7; (b) (●) 0.8; (■) 0.9, and (▲) 0.95. Apparent exposed area of electrode = 2 cm^2.

to a Warburg impedance that is associated with diffusion of lithium ions through the oxide electrode.

As the lithium content of the oxide electrodes increases, the magnitudes of the high-frequency arc in both $Li_{1-\delta}NiO_2$ and $Li_{1-\delta}CoO_2$ remain nearly constant, regardless of the lithium content below $1-\delta=0.8$. The temperature dependence of the impedance spectra was measured in order to investigate which part of the impedance corresponds to intercalation of lithium ions into the electrode, such as charge-transfer or absorption reactions. The change in the diameter of the first arc with temperature gave a value of 10^{-4} eV for the activation energy. This value is too small to be considered as that for the charge-transfer reaction. The magnitude of the high-frequency arc increases with increasing mass of the oxide electrode, but decreases with increasing content of the carbon used for the current collector. This suggests that the high-frequency arc in both $Li_{1-\delta}NiO_2$ and $Li_{1-\delta}CoO_2$ represents particle-to-particle contact resistance and capacitance among the oxide particles.

The values of capacitance associated with the high-frequency and intermediate-frequency arcs were determined from the magnitudes and peak frequencies of the respective arcs. The capacitance for the intermediate-frequency arc is about 2 to 3 orders of magnitude larger than that for the high-frequency arc. This means that a layer with a high concentration of lithium ions exists near the surface region of the oxide electrode, and that lithium ions are adsorbed in a quasi two-

dimensional manner near the surface region of the oxide, as suggested by Conway [14].

Based upon the Conway model [14], the intermediate-frequency arc in the Nyquist plot is related closely to the absorption into the oxide of lithium ions that are adsorbed on the oxide surface. As the lithium content increases up to $1-\delta=0.7$, the absorption resistance for the $Li_{1-\delta}NiO_2$ electrode decreases; it then increases at higher lithium contents. The decrease in the absorption resistance for lithium contents between 0.5 and 0.7 indicates that lithium absorption into the oxide is progressively facilitated by the increased concentration of electrons near the surface region of the oxide electrode. For the higher lithium content range of $1-\delta>0.7$, the increase in absorption resistance is caused by a decrease of the empty sites that are available for the absorption of lithium ions into the oxide electrode. As shown for $Li_{1-\delta}NiO_2$ (Fig. 3), the decrease of lattice constant c with lithium content is small. Therefore, the absorption reaction of lithium ions into the electrode is scarcely affected by the change of lattice parameter.

By contrast, the magnitude of the intermediate-frequency arc associated with the absorption reaction of $Li_{1-\delta}CoO_2$ increases with lithium content. The reverse tendencies for the absorption reactions of lithium ions into $Li_{1-\delta}NiO_2$ and $Li_{1-\delta}CoO_2$ with lithium content are possibly related to the variation of lattice constant c of the two oxides with lithium content. As shown in Fig. 3, the decrease of lattice constant c with lithium content is large for $Li_{1-\delta}CoO_2$. Therefore, the resistance for the absorption reaction increases with lithium content.

3.5. Variation of chemical and component diffusivities with lithium content

The chemical diffusivities of lithium ions in the oxide electrodes were calculated by using Eq. (1) as a function of intercalated lithium content from galvanostatic intermittent titration curves (Fig. 2(a) and (b)) [15]:

$$\tilde{D}_{Li^+}=\frac{4}{\pi}\left(\frac{V_m}{SF}\right)^2\left[\frac{I_0\left(\frac{dE}{d\delta}\right)}{\left(\frac{dE}{d\sqrt{t}}\right)}\right]^2 \quad (1)$$

where $\tilde{D}_{Li^+}$ is the chemical diffusivity of the lithium ion ($cm^2\ s^{-1}$), V_m the molar volume ($cm^3\ mol^{-1}$), I_0 the current (A), S the geometric apparent area of the sample–electrolyte interface (cm^2), F the Faraday constant, $dE/d\delta$ the slope of the coulometric titration curve, and $dE/d\sqrt{t}$ is the slope of the E versus square root of time curve.

The chemical diffusivities of lithium ions in the $Li_{1-\delta}NiO_2$ and $Li_{1-\delta}CoO_2$ electrodes were calculated to be the order of 10^{-8} to $10^{-9}\ cm^2\ s^{-1}$. Considering thermodynamic enhancement factors obtained from the coulometric titration curve, the component diffusivities of the lithium ions, $D_{Li^+,k}$, in the oxide electrodes were calculated from Eq. (2) [15], i.e.:

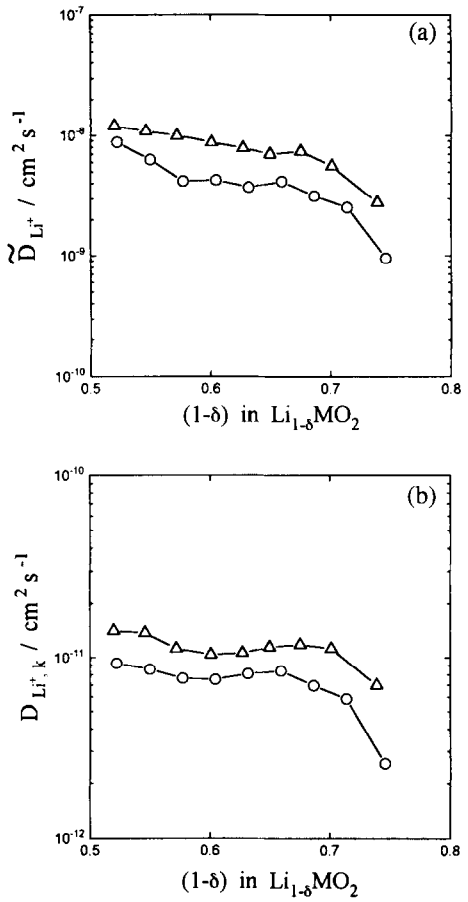

Fig. 6. (a) Chemical diffusivity, $\tilde{D}_{Li^+}$, and (b) component diffusivity, $D_{Li^+,k}$, in (○) $Li_{1-\delta}NiO_2$ and (△) $Li_{1-\delta}CoO_2$ electrodes as function of lithium content, $1-\delta$, at room temperature.

$$D_{Li^+,k}=-\frac{RT}{(1-\delta)F}\left(\frac{\partial\delta}{\partial E}\right)\tilde{D}_{Li^+} \quad (2)$$

where R is the gas constant, T the absolute temperature, and $-[RT/(1-\delta)F](\partial\delta/\partial E)$ is the inverse of the thermodynamic enhancement factor.

The chemical and component diffusivities of lithium ions in the oxide electrodes are plotted in Fig. 6(a) and (b) as a function of lithium content. The chemical and component diffusivities of $Li_{1-\delta}NiO_2$ and $Li_{1-\delta}CoO_2$ vary in a similar manner with lithium content. As the lithium content $(1-\delta)$ increases from 0.5 to 0.8, the value of the chemical diffusivity decreases slightly. The component diffusivity of lithium ions in the oxide electrodes has a nearly constant value of the order of $10^{-11}\ cm^2\ s^{-1}$ in either $Li_{1-\delta}NiO_2$ or $Li_{1-\delta}CoO_2$ at room temperature, irrespective of the lithium content $(1-\delta)$ in the range 0.5–0.7.

The component diffusivity, $D_{Li^+,k}$, is a measure of the random motion of lithium ions in the absence of a concentration gradient, and is expected to be influenced largely by two factors: (i) the number of next empty sites available for lithium ions jumping within the oxide lattice and (ii) the change in lattice constant c of the layered oxide lattice that is caused by intercalated lithium ions.

Assuming that all sites have an equal probability of being occupied, the component diffusivity is expected to decrease linearly with increasing lithium content in the oxide electrode. On the other hand, the lattice constant c of the oxide is reduced by the intercalated lithium ions. This diminishes the width of the path that connects the intercalation sites in the van der Waals gap, and hence lowers the lithium-ion mobility.

Given the variation of the lattice constant c of the layered oxide with lithium content (Fig. 3), the transport of lithium ions through both the layered oxides is not influenced by the change of lattice parameter, but by the number of vacant sites that are available for lithium ions within the lithium-ion layer.

4. Conclusions

Examination of XRD patterns and EIS at various lithium contents, as well as GITT curves of $Li_{1-\delta}NiO_2$ and $Li_{1-\delta}CoO_2$ electrodes in 1 M $LiClO_4$/PC solution has yield the following information.

1. $Li_{1-\delta}NiO_2$ displays a larger loss in capacity during the first intermittent discharge, as well as a greater resistance for the electrochemical intercalation reaction, as compared with $Li_{1-\delta}CoO_2$. This is attributed to a partial cation mixing in $Li_{1-\delta}NiO_2$.

2. The contribution of the coulombic attraction energy to the decreased lattice parameter c during intercalation of lithium into $Li_{1-\delta}CoO_2$ and $Li_{1-\delta}NiO_2$ is predominant over that of elastic strain energy. This may be accounted for in terms of ionic bonding between the transition metal ions and the oxygen ions. The lattice parameter c of $Li_{1-\delta}CoO_2$ decreases more markedly than that of $Li_{1-\delta}NiO_2$ as lithium intercalates into the electrode. This has been discussed in terms of a partial cation mixing in the latter electrode.

3. EIS reveal that the resistance for the absorption of lithium ions into $Li_{1-\delta}NiO_2$ decreases with increasing lithium content. By contrast, the absorption resistance of $Li_{1-\delta}CoO_2$ exhibits the reverse behaviour. The former is largely related to the presence of adsorbed lithium ions on the $Li_{1-\delta}NiO_2$ surface; the latter is mainly associated with a decrease in the lattice constant c of $Li_{1-\delta}CoO_2$ with increasing lithium content.

4. The component diffusivity of lithium ions has a nearly constant value in the order of 10^{-11} cm^2 s^{-1} in both $Li_{1-\delta}NiO_2$ and $Li_{1-\delta}CoO_2$ at room temperature, irrespective of the lithium content, $1-\delta$, in the range 0.5–0.7. This suggests that the transport of lithium ions through the layered oxide electrodes is not influenced by the change in the lattice parameter, but rather by the number of vacant sites within the lithium-ion layer.

Acknowledgements

The receipt of research grant under the programme 'Development of technology of high performance batteries for electric vehicle applications 1992/1993' from the Ministry of Commerce and Industry, South Korea, is gratefully acknowledged. The Korea Research Institute of Standards and Science also financially supported this work under the programme 'A study on lithium anode for high energy density rechargeable batteries 1993/1994'.

References

[1] M.B. Armand, in D.W. Murphy, P.J. Wiseman and J.B. Goodenough (eds.), *Materials for Advanced Batteries*, Plenum, New York, 1980, p. 145.
[2] K.M. Abraham, *Electrochim. Acta, 38* (1993) 1233.
[3] P. Hagenmuller, *Solid State Ionics, 51* (1992) 187.
[4] J.R. Dahn, U. von Sacken, M.W. Juzkow and H. Al-Janaby, *J. Electrochem. Soc., 138* (1991) 2207.
[5] J.R. Dahn, U. von Sacken and C.A. Michal, *Solid State Ionics, 44* (1990) 87.
[6] T. Ohzuku, A. Ueda, M. Nagayama, Y. Iwakoshi and H. Komori, *Electrochim. Acta, 38* (1993) 1159.
[7] T. Ohzuku, A. Ueda and M. Nagayama, *J. Electrochem. Soc., 140* (1993) 1862.
[8] K. Mizushima, P.C. Jones, P.J. Wiseman and J.B. Goodenough, *Mater. Res. Bull., 15* (1980) 783.
[9] M.G.S.R. Thomas, P.G. Bruce and J.B. Goodenough, *J. Electrochem. Soc., 132* (1985) 1521.
[10] J.N. Reimers and J.R. Dahn, *J. Electrochem. Soc., 139* (1992) 2091.
[11] S. Bach, J.P. Pereira-Ramos, N. Baffier and R. Messina, *J. Electrochem. Soc., 137* (1987) 1042.
[12] N. Kumagai, I. Ishiyama and K. Tanno, *J. Power Sources, 20* (1987) 193.
[13] C. Delmas, M.S. Dresselhaus (eds.), *Intercalation in Layered Materials, NATO. ASI. B, 148* (1986) 155.
[14] B.E. Conway, *J. Electrochem. Soc., 138* (1991) 1539.
[15] W. Weppner and R.A. Huggins, *J. Electrochem. Soc., 124* (1977) 1569.